Protein Expression and Purification 90 (2013) 55–66

Contents lists available at SciVerse ScienceDirect

Protein Expression and Purification

journal homepage: www.elsevier.com/locate/yprep

Periplasmic expression optimization of VEGFR2 D3 adopting response surface methodology: Antiangiogenic activity study

Wanlu Cao [1], Haixin Li [1], Juan Zhang *, Daojuan Li, Desmond Omane Acheampong, Zhiguo Chen, Min Wang *

State Key Laboratory of Natural Medicines, China Pharmaceutical University, Nanjing 210009, PR China
School of Life Science & Technology, China Pharmaceutical University, Nanjing 210009, PR China

ARTICLE INFO

Article history:
Received 31 January 2013
and in revised form 26 April 2013
Available online 13 May 2013

Keywords:
Response surface methodology
Periplasmic expression
VEGFR2 D3
Antiangiogenic activity
VEGF blocker

ABSTRACT

Vascular endothelial growth factor (VEGF) is one of the most significant mediators of angiogenesis, which interacts with a specific membrane receptor: VEGF receptor 2 (VEGFR2). Studies elsewhere have shown that, a VEGF-blocker can regulate several vital processes of tumor promotion. However, there is no literature evidence of investigation on antiangiogenic ability of single domain 3 of VEGFR-2 (VEGFR2 D3), as the key domain in signal transduction of VEGF. In this article, we aimed at developing an efficient method for producing soluble form of this receptor as therapeutic applications. The optimization of the production of soluble VEGFR2 D3 in *Escherichia coli* was firstly done by testing the periplasmic expression in different expression systems using three osmotic shock methods. To enhance the yield, vital factors were selected from nine factors by Plackett–Burman design and the level of each viral factor was optimized via a response surface methodology based central composite design. After purification and identification of the protein, the bioactivity assays: quantitative ELISA, VEGF-induced proliferation and *in vivo* chick chorioallantoic membrane assay were employed in our study. The outcome showed that, *E. coli* Rosetta-gami (DE3)/pET22b-VEGFR2 D3 was the most effective expression system. Furthermore, the inducing time, peptone and glycerol concentration affected the periplasmic expression of VEGFR2 D3 significantly. The corresponding level was also optimized. The bioactivity assay studies showed VEGFR2 D3 could suppress both VEGF stimulated cell proliferation *in vitro* and neovascularization *in vivo*. We have therefore provided a novel antiangiogenic drug candidate relating to VEGF-VEGFR2 pathway.

Introduction

Angiogenesis is a precise and complex pathophysiological process in which pre-existing endothelial cells must break through the basement membrane, migrate and proliferate, corresponding to sundry angiogenic factors. Every step of the process is the result of a highly controlled balance of positive or negative modulators, which are secreted by different cell types or cell membrane adhesion molecules [1].

Vascular endothelial growth factor (also known as VEGF-A)[2] is one of the most significant mediators of angiogenesis. It interacts with a specific membrane receptor: vascular endothelial growth factor receptor 2 (VEGFR2) which expresses in most adult vascular endothelial cells and circulating endothelial progenitor cells. The VEGF-VEGFR2 interaction can activate several intracellular pathways, containing endothelial cell proliferation, migration, differentiation, tube formation, vascular permeability increase and the promotion of integrity [2]. The human VEGFR-2 gene encodes 1356 amino acids, including an extracellular region with seven immunoglobulin-like (7-Ig) domains. Among the seven domains, domains 1–3, domain 3 and domains 5 have been proven to be vital in the VEGF-related signal transduction [3].

VEGF blockers have been researched over decades, which promoted antiangiogenic activity by increasing their affinity with VEGF [4–6]. The blocker can regulate several important processes of tumor promotion and progression, which have been implicated in metastatic colorectal cancer, non-small cell lung cancer, glioblastoma multiforme and vascular eye diseases, notably the wet or neovascular form of age-related macular degeneration (AMD) [7].

However, there is no literature investigation on the pharmacological inhibition ability of single domain 3 of VEGFR-2 (VEGFR2 D3), which is the key domain in the signal transduction of VEGF.

* Corresponding authors. Address: State Key Laboratory of Natural Medicines, China Pharmaceutical University, 154#, Tong Jia Xiang 24, Nanjing 210009, PR China. Fax: +86 25 83271395 (J. Zhang).
E-mail addresses: juancpu@126.com (J. Zhang), minwang@cpu.edu.cn (M. Wang).

[1] These authors contributed equally to this work.

[2] *Abbrevation used:* VEGF-A, Vascular endothelial growth factor; VEGFR2, vascular endothelial growth factor receptor; AMD, age-related macular degeneration; EGF, Epidermal growth factor; FGF, fibroblast growth factors; TNF-α, tumor necrosis factor-α; IFN-γ, interferon-γ; BSA, Bovine serum album; PCR, polymerase chain reaction; TBS, Tris-buffered saline.

1046-5928/$ - see front matter © 2013 Elsevier Inc. All rights reserved.
http://dx.doi.org/10.1016/j.pep.2013.04.010

Considering the therapeutic potential of VEGFR2 D3, we sought to develop an efficient and reliable method for producing recombinant VEGFR2 D3 and investigated its potential as a novel antiangiogenic drug candidate relating to VEGF-VEGFR2 pathway.

Material and method

Bacterial strains and plasmids

A strain of *Escherichia coli* (*E. coli*) BL21 (DE3)/pET32a-VEGFR2 D3 preserved in our laboratory was used as the host strain of the VEGFR2 D3 gene. The VEGFR2 D3 gene was cloned into the expression vector pET22b (+) (Novagen).

Reagents

Chemicals, yeast extracts and tryptone were purchased from Merck (Germany); ampicillin was from Sigma (Germany); and isopropyl-β-D-thiogalactopyranoside (IPTG) was from Cinnagen (Iran). Epidermal growth factor (EGF), fibroblast growth factors (FGF), tumor necrosis factor-α (TNF-α) and interferon-γ (IFN-γ) were purchased from SBI (Sino Biological Inc., China). Bovine serum album (BSA) was purchased from Sangon Biotech Inc. (China). Others were marked in passages directly.

Subcloning of the VEGFR2 D3 gene and construction of pET22b-VEGFR2 D3

The VEGFR2 D3 gene (Genebank accession No. AF035121) without signal peptide was inserted into a vector of pET22b (+) (Novagen). First, the VEGFR2 D3 gene was obtained by polymerase chain reaction (PCR) conducted in a 50 μl reaction mixture, each containing 2 μl culture of *E. coli* BL21(DE3)/pET32a-VEGFR2 D3 as template, 1 unites of Taq DNA polymerase (Thermo), 5 μl 10× buffer, 2.5 mM of each dNTP, and 20 pmol of the following primers: upstream primer: 5′-CCG GAA TTC (*Eco*RI) TGT GCT GTT CTT CTT GG-3′, downstream primer: 5′-CCG CTC GAG (*Xho*I) GGT AGA ATT TTT CTT CGT CAT-3′. Then, the recombinant vector of pET22b-VEGFR2 D3 was transferred into *E. coli* DH5α. To confirm the structure of new recombinant plasmid, restriction endonuclease digestion and DNA sequencing were carried out.

Comparison of four VEGFR2 D3 expression systems

The optimization of the production of soluble VEGFR2 D3 in *E. coli* was done by testing different expression systems. Both pET22b-VEGFR2 D3 and pET32a-VEGFR2 D3 plasmids were transformed into *E. coli* Rosetta-gami (DE3) and *E. coli* BL21 (DE3) separately, adopting the Ca^{2+} method [8]. The pET system manual (Novagen) was used as reference to express the recombinant protein in the following four expression systems: *E. coli* Rosetta-gami (DE3)/pET22b-VEGFR2 D3, *E. coli* Rosetta-gami (DE3)/pET32a-VEGFR2 D3, *E. coli* BL21 (DE3)/pET22b-VEGFR2 D3 and *E. coli* BL21 (DE3)/pET32a-VEGFR2 D3.

To evaluate whether the target protein was expressed successfully, a signal clone was inoculated in Luria–Bertani (LB) broth with corresponding antibiotics and a shock at 37 °C for 12–16 h (OD_{280} > 1.0) for each of the four expression systems separately. A starter culture was then transferred into 100 ml Erlenmeyer flasks with 20 ml LB broth containing antibiotics. The culture was induced with 1 mM IPTG at 37 °C to express the target protein. The negative control test was carried out with the recombinant strain without adding inducer. Finally, 40 μl of each culture was harvested and tested for protein expression by sodium dodecyl sulfate polyacrylamide gel electrophoresis (SDS–PAGE). The gel was stained with 0.1% (W/V) Commassie's Brilliant Blue R-250 and analyzed with a gel image system (Bio-Rad).

To confirm whether it contains soluble expression, two hundred milliliter (200 ml) of the culture was centrifuged at 8000 rpm for 15 min at 4 °C. Then, the collected cell pellet was suspended in 10 ml of cell lysis buffer (50 mM Tris–HCl, 0.5 M NaCl, 1% Triton X-100 and at pH 8.0) with appropriate lysozyme. The mixture was then centrifuged at 14,000 rpm for 30 min at 4 °C to get the supernatant as soluble expression protein after sonication (10 min). Finally, SDS–PAGE was adopted to test the soluble expression.

Localization of VEGFR2 D3 in different fractions

The analysis of the expression location of target protein was done by preparing four cell fractions according to the following four steps. Firstly, 200 ml culture was centrifuged at 10,000 rpm for 15 min at 4 °C. The supernatant was then collected as secretary expression. Secondly, the residue was suspended in 10 ml of hypertonic solution (50 mM Tris–HCl, 18% sucrose, 0.1 mM EDTA, and pH 8.0) for 10 min, and centrifuged at 10,000 rpm for 30 min to collect supernatant A. The residue was re-suspended in 10 ml hypotonic solution (5 mM $MgSO_4$) for 10 min, and centrifuged at 10,000 rpm for 30 min to collect supernatant B. The supernatants A and B were mixed, and NaCl added to reach the final concentration of 1.5 M, as the periplasmic fraction. Thirdly, the cell pellet was re-suspended with 20 ml of cell lysis buffer (50 mM Tris–HCl, 0.5 M NaCl, 1% Triton X-100 and pH 8.0) and appropriate lysozyme added. After 10 min sonication, the mixture was then centrifuged at 4 °C for 30 min at 14,000 rpm to collect the supernatant as soluble cytoplasmic fraction. Finally, the residue was dissolved in 10 ml of 8 M urea buffer for 6 h as an inclusion body fraction. All these different fractions were analyzed by SDS–PAGE, followed by Coomassie brilliant blue R-250 staining.

Osmotic shock method

In order to get periplasmic soluble protein, three osmotic shock methods were compared. Since several researchers investigated the optimization of osmotic shock method [9,10], our research focused on the optimized method's practical usage. The details of the three methods are listed in Fig. 1. Method A is an optimized method reported by Ramakrishnan [9]. Method B is a simplified method published by Shouchun Cao [10]. Method C is another method optimized by our laboratory. The main difference between the three methods lies in hypertonic solution and hypotonic solution. The evaluation standards were recorded in two parts: (1) the target protein's yield and (2) the entire collected periplasmic protein's yield. The entire protein yield was tested by Bradford protein assay and the target protein's percentage was obtained by the Automatic Analysis System of Electrophoresis Gel Imaging (Bio-Rad). The target protein's yield equaled the target protein's percentage multiply by the entire collected periplasmic protein's yield. All experiments were repeated three times to gain the average.

Plackett–Burman design (PBD)

The optimization of the periplasmic expression of VEGFR2 D3 in *E. coli* Rosetta-gami (DE3) was done by employing PBD [11,12]. Nine variables were carefully selected and evaluated by PBD with twelve experiments. These variables were: induction time, induction temperature, rotational speed after induction, IPTG (inducer) concentration, glycerol concentration, yeast and peptone concentration, NaCl concentration and ammonium sulfate. The experiments were designed and analyzed with the software package "Minitab 15" (Minitab Inc). The PB experiments contained a total

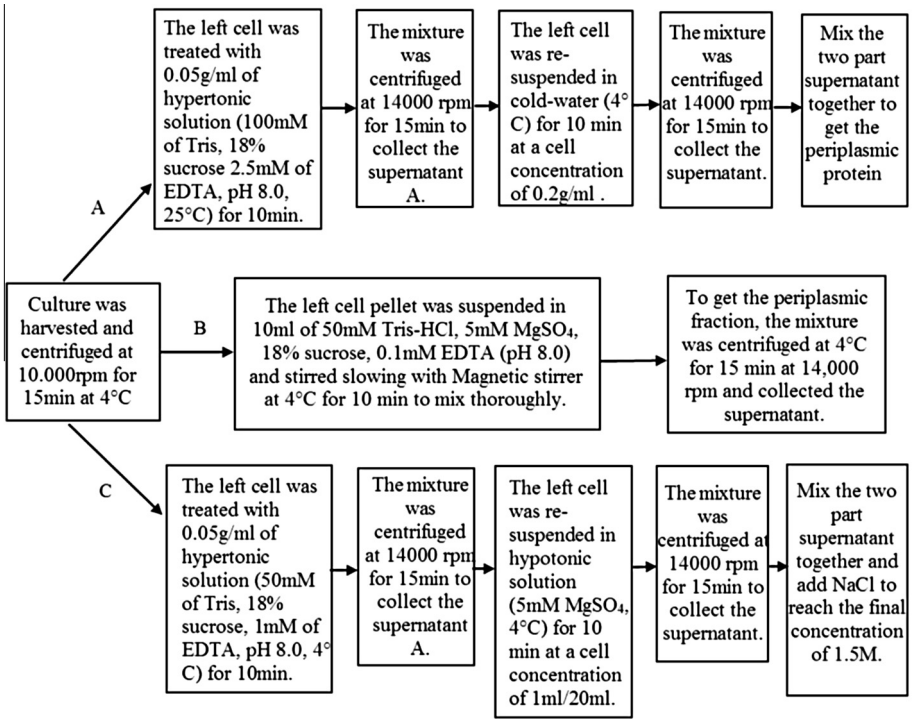

Fig. 1. The details of three osmotic shock methods.

of 12 experimental trials. Each variable was tested at two levels: −1(low level) and +1(high level). The practical levels were obtained from previous work in the laboratory, and the difference between the two values should be large enough to ensure the peak area for protein's expression [13]. For each two factors, there were four different combinations and three-time repetition for each of the combinations. The practical PBD matrixes for all nine variables and the detail of the design are given in the Table 1. The response was the yield of VEGFR2 D3, which was calculated as mentioned above (conducted in triplicates to gain average).

Experimental design and statistical analysis: central composite design (CCD)

In order to explore the optimization more comprehensively, a design with more than two levels should be carried out [14]. Therefore, a response surface methodology (RSM) based on the CCD was chosen to obtain optimized levels of glycerol concentration, inducing time and peptone concentration. The three factors were selected by PBD on the expression level of periplasmic protein in *E. coli* Rosetta-gami (DE3) [13]. The software package "Minitab 15" (Minitab Inc.) was taken to design the experiment. Each factor was tested at five levels: +1.68179(+α), +1 (the higher value of the factors), 0(central point), −1(the lower value of the factors) and −1.68179(−α). The level 0 of each factor was the optimized level from previous PBD, and the difference between the five values should be significant enough to ensure the peak area for protein's expression. The design consisted with a central composite design with six replications of the central points (all factors' level at 0) and the six star points (which means one factor an axial distance to the centre of ±α and other two factors are at level 0). The relationships and interrelationships of glycerol concentration, inducing time, and peptone concentration were evaluated by fitting the second order polynomial equation to data obtained from 20 experiments. The experimental design matrix was given in Table 2 and values of different variables and practical levels in the central composite design were described in Table 3. All experiments were carried out in triplicates. The significance of each linear effect and

Table 1
The Placket–Burman experimental design of 12 run with 9 variables and the response (the target protein's yield).

Std ID	Factor A yeast concentration (g/L)	Factor B temperature (°C)	Factor C Glycerin (%)	Factor D inducing time (h)	Factor E rotation speed (rpm)	Factor F inducer concentration (mM)	Factor G ammonium sulfate (g/L)	Factor H NaCl (g/L)	Factor J peptone concentration (g/L)	Response 1 VEGFR2 D3 product concentration(ng/L)
1	10	37	0	20	220	0.05	10	0.05	1	1020
2	10	16	2	20	150	1	0	0.05	1	1440
3	1	37	2	5	220	0.05	0	0.05	10	1400
4	1	37	0	5	150	1	10	10	1	350
5	10	16	0	5	220	1	10	0.05	10	860
6	10	37	2	5	220	1	0	10	1	890
7	1	16	0	20	220	1	0	10	10	1430
8	1	37	2	20	150	1	10	0.05	10	1560
9	1	16	0	5	150	0.05	0	0.05	1	590
10	10	16	2	5	150	0.05	10	10	10	1440
11	10	37	0	20	150	0.05	0	10	10	1510
12	1	16	2	20	220	0.05	10	10	1	1190

Table 2
Experimental designs used in CCD studies by using three independent variables with six center points showing actual values of VEGFR2 D3 yield (response).

Run	Factor A glycerin (%)	Factor B inducing time (h)	Factor C peptone concentration (g/L)	Response 1 VEGFR2 D3 product concentration(μg/L)
1	0	0	0	1908
2	−1	1	1	1584
3	0	0	0	1956
4	−1	−1	1	1464
5	0	0	0	1980
6	−1	1	−1	1788
7	1	−1	−1	1572
8	0	0	0	1836
9	1	1	−1	1704
10	0	0	0	1812
11	1	−1	1	1176
12	0	0	1.68179	1584
13	1.68179	0	0	1716
14	0	0	−1.68179	1776
15	−1	−1	−1	1668
16	0	1.68179	0	1344
17	−1.68179	0	0	1824
18	0	−1.68179	0	876
19	0	0	0	2064
20	1	1	1	1608

Table 3
Experimental range of the three variables studied using central composite design in terms of actual and coded factors.

Variable levels	Component	Level				
		−1.6817	−1	0	+1	+1.6817
A	Glycerol concentration	1.6%	3%	5%	7%	8.4%
B	Inducing time	11.6 h	15 h	20 h	25 h	28.4 h
C	Peptone concentration	6.6 g/L	10 g/L	15 g/L	20 g/L	21.6 g/L

interactions were determined with the student's *t*-test, and the test was performed at 0.1 level [15].

Purification of VEGFR2 D3 protein

Nickel affinity column was used to purify the target protein considering the fact that the recombinant VEGFR2 D3 has a His-tag. The details are described as following. First, 0.22 μl filter was used to filter the periplasmic collection. The Ni affinity column was then set up and pre-equilibrated with 10 bed volume of binding buffer (20 mM carbonate, 25 mM imidazole, pH 10.0, and 4 °C). The sample was then loaded by a pump (Bio-red) at the flow rate of 0.45 ml/min. The column was then washed with 10 bed volume of binding buffer. To collect the target protein, the column was eluted with 150 mM imidazole. Finally, the purity of VEGFR2 D3 was determined by high performance liquid chromatography (HPLC) on an Agilent 1200 system equipped with a TSK-GELG4000PW$_{XL}$ column. Taking phosphate buffer solution (PBS, pH 7.4) as the mobile phase, VEGFR2 D3 (50 μg) was dissolved in 0.5 ml PBS and injected in each run at a flow rate of 0.5 ml/min. Absorbance at 280 nM was continuously monitored [16].

Protein identification with Western blotting (WB)

WB was adopted for the preliminary identification of recombinant VEGFR2 D3. The purified proteins were loaded into the 15% SDS–PAGE gel with three concentrations (50 μg/ml, 100 μg/ml and 200 μg/ml) and then transferred onto the polyvinylidene fluorid (PVDF) membranes (Millipore). This membrane-transference was carried out for 1.5 h in a blotting apparatus (Bio-Rad) under a constant voltage at 100 V. After blotting, 5% fat-free milk in Tris-buffered saline (TBS, pH 7.4) was used as blocking solution at 37 °C for 2 h. The membrane was then washed three times with TBS before incubating with His-Tag Mouse mAb (1:2000, Cell Signaling, 27E8) overnight at 4 °C. After washing three times with TBST(TBS containing 0.05% Tween-20) and three times with TBS, the membrane was incubated for 2 h at 25 °C with Goat Anti-Mouse IgG∗HRP (1:5000, MultiSciences Biotech, 11-GAM007). Finally, the blots were treated with enhanced chemiluminescence (ECL) solution (Millipore) and developed in gel imaging systems (Bio-rad).

Quantitative enzyme linked immunosorbent assay (ELISA)

Protein-binding ELISA plate (JEF BIOFIL) was used in the ELISA assay. 100 μl of diluted VEGF$_{165}$ (1000 nM, dissolved in PBS, expressed and purified previously in our lab) was added in each well. BSA, EGF, FGF, TNF-α and IFN-γ were added in each well as negative control separately, which all with a concentration of 1000 nM and dissolved in PBS. After overnight incubation at 4 °C, the coated plates were blocked with 5% fat-free milk for 1. 5 h and then washed with TPBS (PBS containing 0.05% Tween 20) and PBS for three times. Serial dilutions of VEGFR2 D3 (0.9 nM, 1.9 nM, 3.9 nM, 7.8 nM, 15.6 nM, 31.3 nM, 62.5 nM, 125.0 nM, and 250.0 nM) were added into the plate and incubated at 25 °C for another 2 h. TPBS and PBS were used to wash the plate and His-Tag Mouse mAb (1:2000, Cell Signaling, 27E8) was added and incubated for 1.5 h. After washing as described previously, the Goat Anti-Mouse IgG ∗ HRP (1:5000, MultiSciences Biotech, 11-GAM007) was then added into the wells and incubated at 25 °C for 1.5 h. 100 μl of color development solution (0.03% H_2O_2 and 2 mg/ml TMB in 0.1 M NaAc buffer, pH 6.0) was added and the plate was incubated at 25 °C until color emerged after washing with TPBS and PBS each for three times. Finally, the reaction was stopped with 50 μl of 1 M H_2SO_4, and the absorbance was measured at OD_{450}–OD_{650} nM [17].

Cell proliferation assay

Human umbilical vein endothelial cell line (EA.hy926) was used to test the VEGF induced proliferation. The Dulbecco's modified eagle medium (DMEM medium) with 10% fetal bovine serum (FBS, Giboc) was adopted to culture EA.hy926. After incubating for 24 h (37 °C, 5% CO_2), 0.25% trypsin was taken to passage (Invitrogen). EA.hy926 was diluted and plated with 3×10^3 cells/well in a 96-well plate (Corning Costar) and then incubated for another 24 h. Then, VEGF (VEGF$_{165}$, 250 nM) and different concentrations of VEGFR2 D3 (100 nM, 50 nM, 25 nM, 12.5 nM, 6.25 nM, 3.13 nM, and 1.56 nM) were added to each well (n = 3). Wells without VEGF$_{165}$ and VEGFR2 D3 were treated as blank control and wells with added Sunitinib (Pfizer) (100 nM, 50 nM, 25 nM, 12.5 nM, 6.25 nM, 3.13 nM, and 1.56 nM) and VEGF (VEGF$_{165}$, 250 nM) were taken as the positive control. Plus, Wells added with FGF (250 nM) and VEGFR2 D3 or EGF (250 nM) and VEGFR2 D3 were taken as negative control. After 72 h proliferation, 11 μl/well of methyl thiazolyl tetrazolium (MTT) was added and cultivated for 4 h. 150 μl DMSO was added for formazan solubilization after moving the original medium. The absorbance of the solution was measured at 570 nM and 630 nM by a micro-plate reader (Thermo). The IC_{50} was calculated by using SPSS 15(IBM SPSS) [18].

In vivo chick chorioallantoic membrane (CAM) assay

CAM assay was performed as described elsewhere [19]. Groups of 40 fertilized chicken eggs (Nanjing Medical Device Factory) were incubated at 37 °C with 55% relative humidity. After six-day cultivation, a medical small bending shear and curved forceps were used to open a window 1 cm^2 over the dropped CAM. Filter paper

disks saturated with physiological saline, VEGFR2 D3 (10 μM) + VEGF (2 μM), VEGFR2 D3 (500 μM) + VEGF (2 μM), VEGF (2 μM), EGF (2 μM), VEGFR2 D3 (10 μM) + EGF (2 μM), or FGF (2 μM) or VEGFR2 D3 (10 μM) + FGF (2 μM) were placed on avascular area of membranes separately. Then, the embryos were incubated for another 48 h. After a 15 min fixation with 2 ml fixative (methanol-to-acetone, 1:1), each piece of membrane was carefully transferred to a cover slip, and the vascular zones under the disks were photographed. Angiogenesis or antiangiogenesis was quantified by counting the number of blood vessel branch points. The assay was repeated three times to ensure the reproducibility.

Results

The construction and comparison of expression systems

As shown in Fig. 2, the restriction endonuclease digestion and DNA sequencing indicated that the gene of VEGFR2 D3 without signal peptide was successfully obtained by PCR and transferred into a new vector of pET22b (+). Theoretical molecular mass of VEGFR2 D3 expressed with pET22b and pET32a in *E. coli* was 15 kDa (pelB-VEGFR2 D3) and 28 kDa (Trx-VEGFR2 D3) separately. The SDS–PAGE results also showed that the VEGFR2 D3 was successfully expressed under the induction of IPTG or lactose (Fig. 3a Lane 5–7) using the expression system *E. coli* Rosetta-gami (DE3)/pET22b-VEGFR2 D3. It was also expressed successfully in a soluble form as shown in Fig. 3e. The expression system *E. coli* BL21 (DE3)/pET32a-VEGFR2 D3 was effectively used to produce high yield of the target protein as shown in Fig. 3b Lane 5–7. However, the target protein was mostly expressed as an inclusion body as depicted in Fig. 3c. In the case of the strain *E. coli* Rosetta-gami (DE3)/pET32a-VEGFR2 D3 system, the protein was successfully expressed in the soluble form as shown in Fig. 3d. Nevertheless, other unwanted proteins were expressed at high concentration, which could affect purification greatly. For strain *E. coli* BL21 (DE3)/pET22b-VEGFR2 D3, no target protein was expressed under the induction of IPTG or lactose (Fig. 3b Lane 1–3).

Localization of VEGFR2 D3 in different fractions

The target protein was mainly expressed as inclusion body as shown in Fig. 4, lane 4. It was also expressed as the secretary protein, periplasmic protein and cytoplasmic soluble expression as shown in Fig. 4, lane 1–3, respectively. There obviously existed a balance between the four forms of expression.

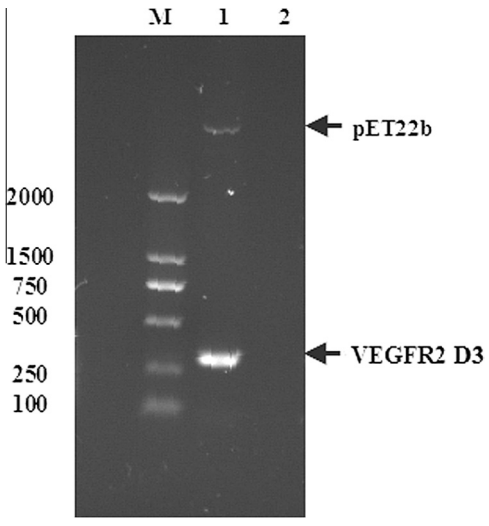

Fig. 2. PCR identification of pET22b-VEGFR2 D3. M: nuclear marker. Lane 1: restriction endonuclease digestion of single colony. Lane 2: negative control (DD water).

Osmotic shock method

The data presented on Table 4 showed that the simplified method (B), which combined the hypertonic solution and hypotonic solution together, also can be used to obtain the periplasmic protein with a high concentration and appropriate-level of impurities. Methods A and C which are all two-step extraction methods enhanced protein impurities, with a slight enhancement in target protein yield.

PBD

PBD is a powerful tool for identifying factors with significant influence on protein's periplasmic expression [15,20]. The evaluation of different culture conditions for the expression of recombinant VEGFR2 D3 derived from *E. coli* Rosetta-gami (DE3) was performed in 500 ml shaking flasks containing 100 ml various cultures under the corresponding incubating condition. The result showed that the nine variables all influenced VEGFR2 D3's periplasmic expression, as depicted in Table 5.

The value for R^2 was 0.9873, which meant the model was capable of explaining 98.73% variability of the data, while only a few fractions of data remained (1.27%) unexplained. The regression analyses data of PBD were shown in Table 5. It revealed that peptone concentration (J), glycerol concentration (C) and inducing time (D) were the critical factors that affected the periplasmic expression of VEGFR2 D3. The variables corresponding to a probability less than 0.1 were considered to be significant [21]. In addition, Pareto chart presented in Fig. 5a revealed that the maximal effect (J: peptone concentration) was presented in the upper portion and then progressed down to the minimal effect (H: NaCl concentration). Furthermore, six other factors that potentially influenced the expression level were monitored. As shown in Fig. 5b, the lower rotation speed, temperature, ammonium sulfate concentration, inducer concentration, and the higher yeast concentration, NaCl concentration could stimulate the expression of soluble periplasmic proteins.

Experimental design and statistical analysis: CCD

Three variables, including glycerol concentration (A), inducing time (B) and peptone concentration (C), which proved to have significant effect on the periplasmic expression by PBD, were required for optimization. So, a second order approximation to the response surface needed to be developed. The central composite design and the corresponding experimental data are shown in Table 2 and 3.

The statistical analysis of the results demonstrated that the inducing time (B), peptone concentration (C) and the B^2 and C^2 had significant influence on expression level (P-value < 0.1). The effect of the inducing time was positive (4.526, $P = 0.001$), indicating that longer inducing time will enhance the expression of periplasmic soluble protein, whereas the peptone concentration was negative (3.479, $P = 0.006$). The interactions between the three variables were not significant. Considering these results, a simplified second-order polynomial equation for VEGFR2 D3 expression in terms of coded factors is presented as the following: $Y = 1923.57 + 116.5\,B - 89.55C - 272.65B^2 - 71.12C^2$.

The response surface plots and their corresponding contour plots described by the second-order polynomial equation were illustrated in Fig. 6. These pictures revealed that the model contained the entire optimum region for VEGFR2 D3 production located at the peak of the surface [22]. The fit of the model was illustrated by determination of a coefficient (R^2). In this case, an

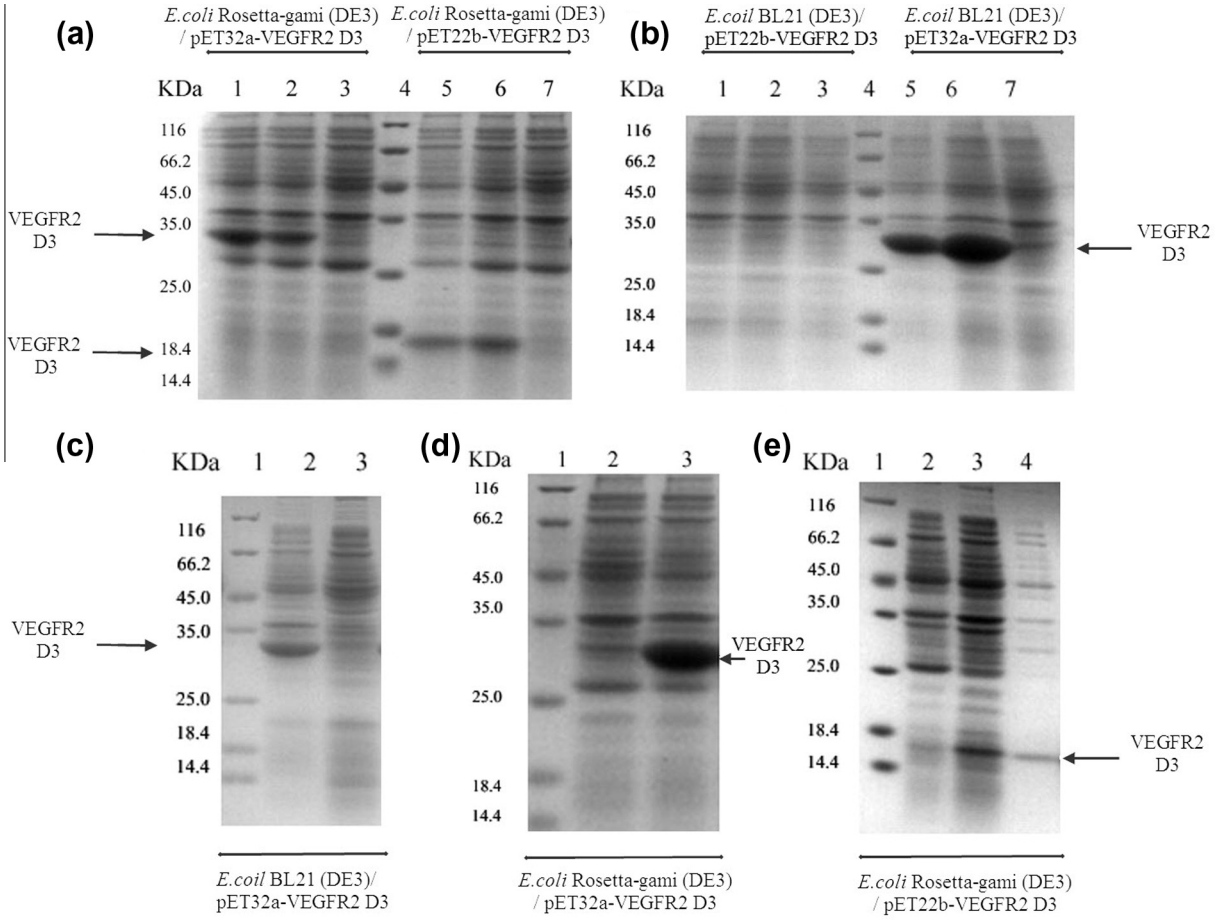

Fig. 3. The SDS–PAGE identification of four expression systems. System A: *E. coli* Rosetta-gami (DE3)/pET32a-VEGFR2 D3; System B: *E. coli* Rosetta-gami (DE3)/pET22b-VEGFR2 D3; System C: *E. coli* BL21 (DE3)/pET22b-VEGFR2 D3; System D: *E. coli* BL21 (DE3)/pET32a-VEGFR2 D3. (a) Lane 1: System A, under the induction of IPTG. Lane 2: System A, under the induction of lactose. Lane 3: System A, negative control. Lane 4: protein marker. Lane 5: System B, under the induction of IPTG. Lane 6: System B, under the induction of lactose. Lane 7: System B, negative control. (b) Lane 1: System C, under the induction of IPTG. Lane 2: System C, under the induction of lactose. Lane 3: System C, negative control. Lane 4: protein marker. Lane 5: System D, under the induction of IPTG. Lane 6: System D, under the induction of lactose. Lane 7: System D, negative control. (c) Lane 1: protein marker. Lane 2: System D, under the induction of IPTG. Lane 3: System D, soluble expression. (d) Lane 1: protein marker. Lane 2: System A, soluble expression. Lane 3: System A, under the induction of IPTG. (e) Lane 1: protein marker. Lane 2: System B, negative control. Lane 3: System B, under the induction of IPTG. Lane 4: System B, soluble expression.

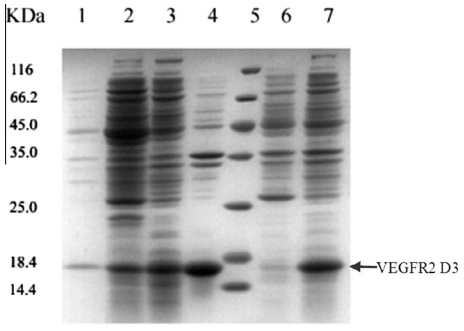

Fig. 4. SDS–PAGE analysis of four fractions of *E. coli* Rosetta-gami (DE3)/pET22b-VEGFR2 D3. Lane 1: secretary fraction. Lane 2: periplasmic expression. Lane 3: cytoplasmic soluble expression. Lane 4: inclusion body. Lane 5: protein marker. Lane 6: negative control. Lane 7: the whole-cell fraction.

R^2 of 0.9412 indicated that 94.12% of the total variability in the response could be well explained by the new model. The statistical significance of the model was evaluated by the *F*-test ANOVA Table 6 and 7, which revealed that this regression was statically significant ($P < 0.05$).

With the prediction of the maximum soluble expression, an optimal design was carried out with the aid of Minitab 15. A maximum periplasmic yield (1.967 mg/L) was predicted at the condition of 4.15% of glycerol concentration, 20.77 h of inducing time and 12.197 g/L of peptone. In order to verify the predicted results, a group of experiments were performed under the optimized levels with a production of 1.989 mg/L (mean result of three repetitions), suggesting that experimental and predicted values of VEGFR2 D3 expression were in good agreement, validating the model.

Purification and identification of VEGFR2 D3 protein

The SDS–PAGE was used to analyze the recombinant VEGFR2 D3 as shown in Fig. 7a. The HPLC result showed that the Ni–NTA could yield the target protein with purity higher than 95% (Fig. 7b). In addition, the WB results exhibited that the expressed VEGFR2 D3 had a molecular weight of 15 KDa, which was the expected figure. His-tag fused on the C-terminal was also successfully expressed (Fig. 7c). The entire results were taken as the preliminary identification of VEGFR2 D3 expression.

Quantitative ELISA assay

The combination ability of the recombinant VEGFR2 D3 with the $VEGF_{165}$ was determined by ELISA. The binding of serial diluted VEGFR2 D3 (0.95 nM, 1.9 nM, 3.9 nM, 7.8 nM, 15.6 nM, 31.3 nM,

Table 4
The outcomes of three osmotic shock methods.

Method	Entire periplasmic protein's yield	The target protein's percentage	The target protein's yield
A	6.73 mg/ml	23%	1.5479 mg/ml
B	2.92 mg/ml	42%	1.2264 mg/ml
C	7.09 mg/ml	19%	1.3471 mg/ml

Table 5
The regression analyses data of PB design with nine variables, analyzed by Minitab 15.

Variables	Actual factors	Coefficient	*F*-Value	*P*-Value
–	Intercept	114.000	37.74	0.001
Factor A	Yeast concentration (g/L)	5.333	1.77	0.220
Factor B	Induction temperature (°C)	−1.833	−0.61	0.606
Factor C	Glycerol concentration (%)	18.000	5.96	0.027**
Factor D	Inducing time (h)	21.833	7.23	0.019**
Factor E	Rotational speed after induction (rpm)	−0.833	−0.28	0.809
Factor F	IPTG (inducer) concentration (mM)	−5.167	−1.71	0.229
Factor G	Ammonium sulfate(g/L)	−7.000	−2.32	0.146
Factor H	NaCl concentration (g/L)	−0.500	−0.17	0.884
Factor J	Peptone concentration (g/L)	22.667	7.50	0.017**

62.5 nM, 125 nM, and 250 nM) to $VEGF_{165}$ (1000 nM) increased gradually. In addition, the negative control group (BSA, EGF, FGF, TNF-α and IFN-γ) exhibited no obvious combination with VEGFR2 D3 as shown in Fig. 8.

Cell proliferation assay

In order to evaluate whether VEGFR2 D3 can restrain the VEGF induced proliferation of EA.hy926, cell counts were measured with MTT assay. As the data indicated in Fig. 9, the proliferation of EA.hy926 was remarkably inhibited by the addition of VEGFR2 D3. Seven doses of VEGFR2 D3 were used in the experiment, showing a dose-dependent inhibition (IC_{50} = 63.937 nM, 0.9591 ng/ml) and owning the same restraining tendency with Sunitinib here. Plus, VEGFR2 D3 had no obvious restriction to EGF-induced proliferation and FGF-induced proliferation.

In vivo CAM assay

In determining if VEGFR2 D3 can suppress blood vessel formation *in vivo*, we adopted an *in vivo* angiogenesis model, the CAM model. With the induction of VEGF (2 μM), the number of new capillary vessels increased obviously, compared to the physiological saline group. In the meantime, VEGFR2 D3 showed significant inhibition. These results indicated that VEGFR2 D3 was capable of inhibiting neovascularization *in vivo*. In addition, VEGFR2 D3 showed no obvious restriction ability in FGF-induced angiogenesis or EGF-induced angiogenesis. Representative photographs of CAM assays and quantitative data are summarized in Fig. 10.

Discussion

Therapeutic angiogenesis is an attractive field of medical research. Our study aimed at preparing an attractive candidate for further development in therapeutic angiogenesis.

The vector of pET22b harbors a pelB signal peptide at the protein N-terminal, leading the protein into the periplasmic space [23]. The plasmid of pET32a has a Trx signal peptide, which can promote soluble expression of recombinant protein in *E. coli* and also protect the target protein from degradation by protease. Among the four construction systems that were used in this study, *E. coli* Rosetta-gami (DE3)/pET22b-VEGFR2 D3 was the most effective and appropriate one. Periplasmic secretion of our protein was achieved because of the presence of pelB signal peptide, which directly leaded the target protein to periplasmic space. This transference has the following advantages: (1) separating from other impurities in cytoplasmic space (2) providing an oxidizing medium benefited in the formation of disulfide bond (3) reducing the protease to keep the target's activity and biological structure [24]. Plus, *E. coli* Rosetta-gami (DE3) can alleviate rare-codon usage basis during the protein's expression. Therefore, the effectiveness of the *E. coli* Rosetta-gami (DE3)/pET22b-VEGFR2 D3 system could be attributed to these features.

The available methods that can be used to release periplasmic proteins are mechanical and physical cell disruption methods. Mechanical methods are known to release protein with low selectivity, which make purification process more difficulty [25]. This informed our decision to use the physical cell disruption method. So, we chose the osmotic shock over the mechanical treatment. Advantages of the osmotic shock are that, it comes with low-cost and high selectivity in protein releasing process. Three of the known osmotic methods were used in this study and came out that method B described in our methodology was the most effective. The possible explanation is that, the stabilization of the outer membrane of the Gram-negative cell envelope requires Mg^{2+} and the fact that EDTA can be chelate with Mg^{2+} to cause the loss of lip polysaccharide, a higher EDTA concentration which was

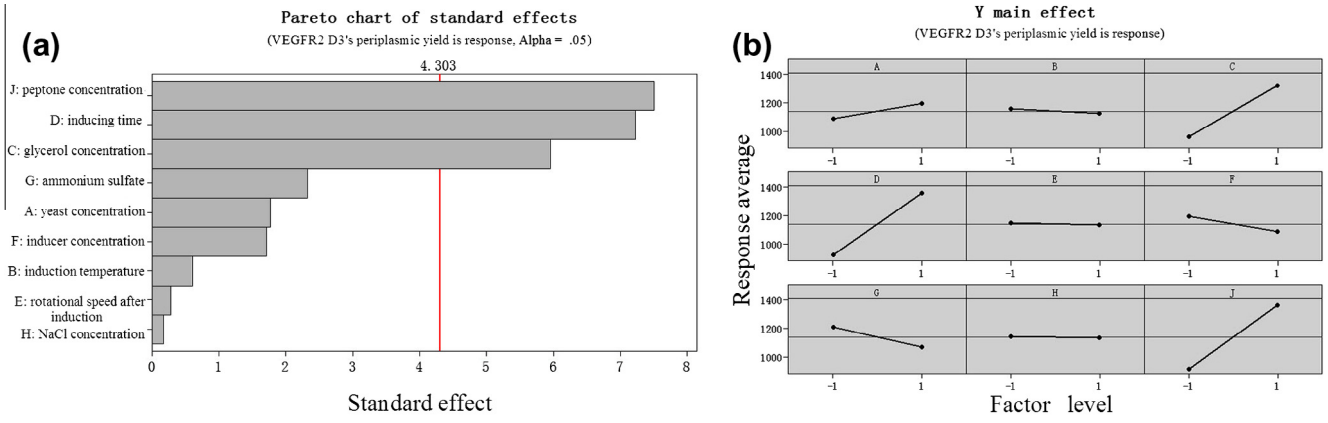

Fig. 5. Pareto chart and influence tendency of each factor. (a) Pareto chart of nine-factor standard effects on target protein's periplasmic yield. The important terms were J (peptone concentration), D (inducing time) and C (glycerol concentration). (b) Factors' influence effect on response. The forward influence: A, C, D and J. The backward influence: B, E, F, G and H. (b) the influence tendency of each factor.

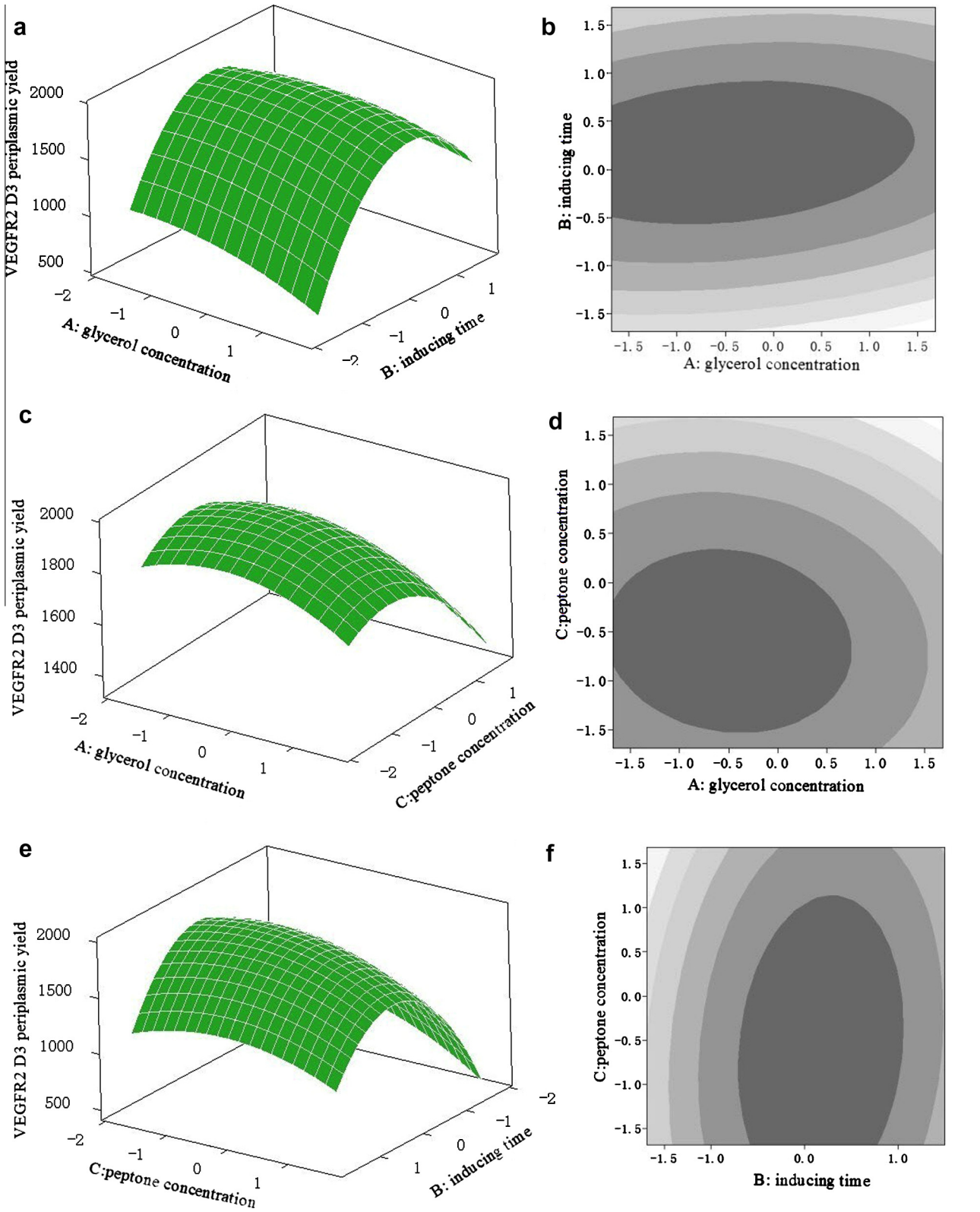

Fig. 6. Response surface plot and its contour plot described by the model Y. (a and b) Shows the effect of glycerol concentration (A) and inducing time (B) on VEGFR2 D3 periplasmic yield (peptone concentration = 15 g/L), (c and d) shows the effect of glycerol concentration (A) and peptone concentration (C) on VEGFR2 D3 periplasmic yield (inducing time = 20 h), (e and f) shows the effect of inducing time (B) and peptone concentration (C) on VEGFR2 D3 periplasmic yield (glycerol concentration = 5%).

employed in methods A and C would cause cell-membrane lysis. This will lead to an enhanced yield of impurities, and therefore make the subsequent purification process more difficult. Also the method B has shorter extraction process. This feature is better for the consideration of protein's biological activity and the economic factor. In general, this one-step extraction can save time and also reduce the purification steps when compared to other two-step osmotic shock methods.

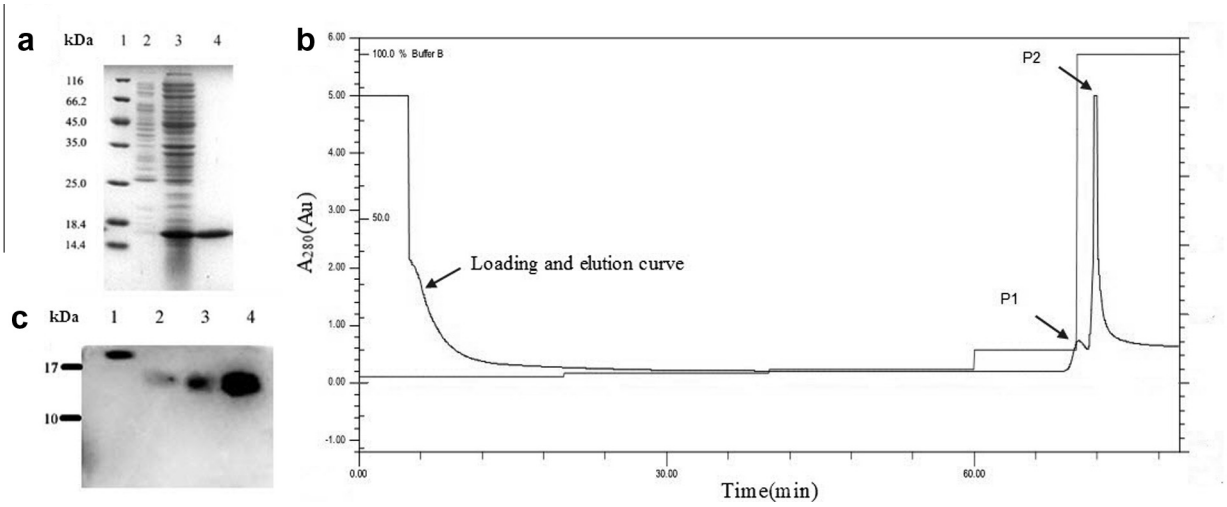

Fig. 7. The identification of the target protein. (a) SDS–PAGE analysis of purification of VEGFR2 D3 with Ni-affinity column. Lane 1: molecular weight marker. Lane 2: negative control (without inducer). Lane 3: the whole cell fraction. Lane 4: purified VEGFR2 D3. (b) HPLC analysis of purified VEGFR2 D3. P1: the impurities (5%). P2: the VEGFR2 D3 (95%). (c) Protein identification by WB. Lane 1: positive control (IL-21, expressed and preserved in our lab). Lane 2: 50 μg/ml VEGFR2 D3. Lane 3: 100 μg/ml VEGFR2 D3. Lane 4: 200 μg/ml VEGFR2 D3.

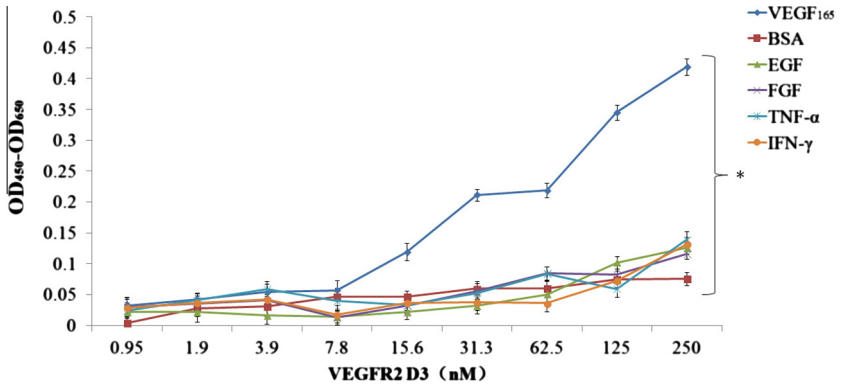

Fig. 8. ELISA assay. The combination between the recombinant VEGFR2 D3 and $VEGF_{165}$ was tested. The combinations of VEGFR2 D3 with BSA, EGF, FGF, TNF-α and IFN-γ were taken as the negative control. Plus, Mean ± SD, $n = 3$. * means ($Pb < 0.05$ vs. control).

Considering the limitation of periplasmic space, a reliable and effective method was required to improve the yield of VEGFR2 D3. Researchers have proven that the culture condition, cultivation media and inducer concentration can affect the periplasmic expression of recombinant protein significantly [15,20,21], and our laboratory evaluated the culture components' influence on the expression of protein in *E. coli* previously. So, five different factors, including the carbon source (yeast and glycerol), inorganic nitrogen source (ammonium sulfate), organic nitrogen source (peptone) and salt ions (NaCl), were selected to research here and the corresponding levels were determined according to the our precious work in laboratory. In addition, the T7 expression system is well recognized as an effective tool for protein overproductions [26]. Considering both of the pET22b and pET32a plasmid all contain T7 promoter, we need to keep balance between the high express level and protein's active form. So, another three culture conditions (induction temperature, rotational speed after induction, inducing time), which other researchers reported that could influence the periplasmic expression, were compared to find out the best combination [27,28]. Another factor that influences the express significantly in the T7 expression system is the inducer concentration. Taking the protein's expression form into consideration, lower concentration of inducer was compared in our study (1 mM, 0.05 mM).

Studies on expression condition that adopt conventional single-factor optimization, which use one variable at one time, do not allow the interaction between different variables. Furthermore, this method is too time-consuming to carry out in an effective way. Since our study involved more than five factors, and PB design had been strongly recommended to be used in such circumstances, we adopted this method in our study. PBD is known to provide indications and tendencies regarding the necessity of each factor just needing relatively few experiments [21]. In other words, PBD allows testing the largest number of factors with the least number of observations, estimating the variability of random error and testing the statistical significance of the parameter. In addition, RSM, as a high effective method, can verify the interactions between the variables [29,30]. Therefore, this method was used to obtain the optimal conditions for desirable responses and also reduced the general number of experiments that we were required to undertake. PBD and CCD were thus carried out to improve our target protein yield.

In this study, the result of PBD indicated that the higher concentration of periplasmic protein was correlated to longer inducing time, higher glycerol concentration and higher peptone concentration significantly. Then, CCD predicted that a maximum periplasmic yield was obtained at the condition of 4.15% of glycerol concentration, 20.77 h of inducing time and 12.197 g/L of peptone.

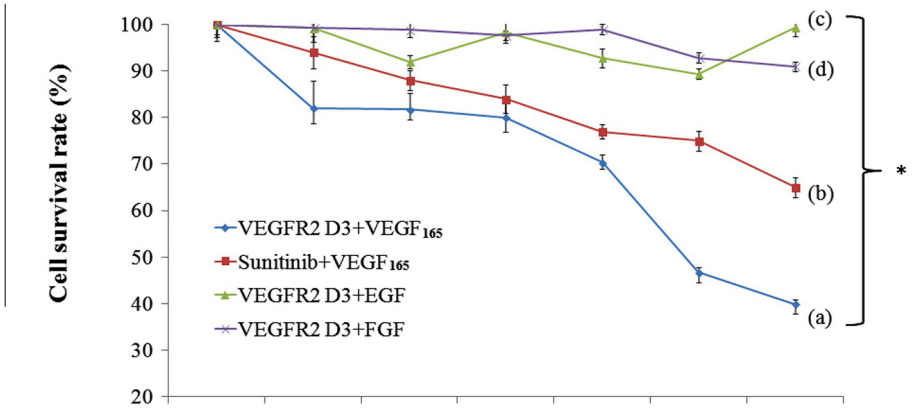

(a)VEGFR2 D3(nM):	1.56	3.13	6.25	12.50	25.00	50.00	100.00
$VEGF_{165}$(250nM):	+	+	+	+	+	+	+
(b) Sunitinib (nM) :	1.56	3.13	6.25	12.50	25.00	50.00	100.00
$VEGF_{165}$(250nM):	+	+	+	+	+	+	+
(c)VEGFR2 D3(nM):	1.56	3.13	6.25	12.50	25.00	50.00	100.00
EGF(250nM):	+	+	+	+	+	+	+
(d)VEGFR2 D3(nM):	1.56	3.13	6.25	12.50	25.00	50.00	100.00
FGF(250nM):	+	+	+	+	+	+	+

Fig. 9. Proliferation assay of VEGFR2 D3. (a) Various concentrations of VEGFR2 D3 + $VEGF_{165}$ (250 nM), (b) various concentrations of Sunitinib + $VEGF_{165}$ (250 nM), (c) various concentrations of VEGFR2 D3 + EGF (250 nM), (d) various concentrations of VEGFR2 D3 + FGF (250 nM). Plus, Mean ± SD, $n = 3$. ∗ means (Pb < 0.05 vs. control).

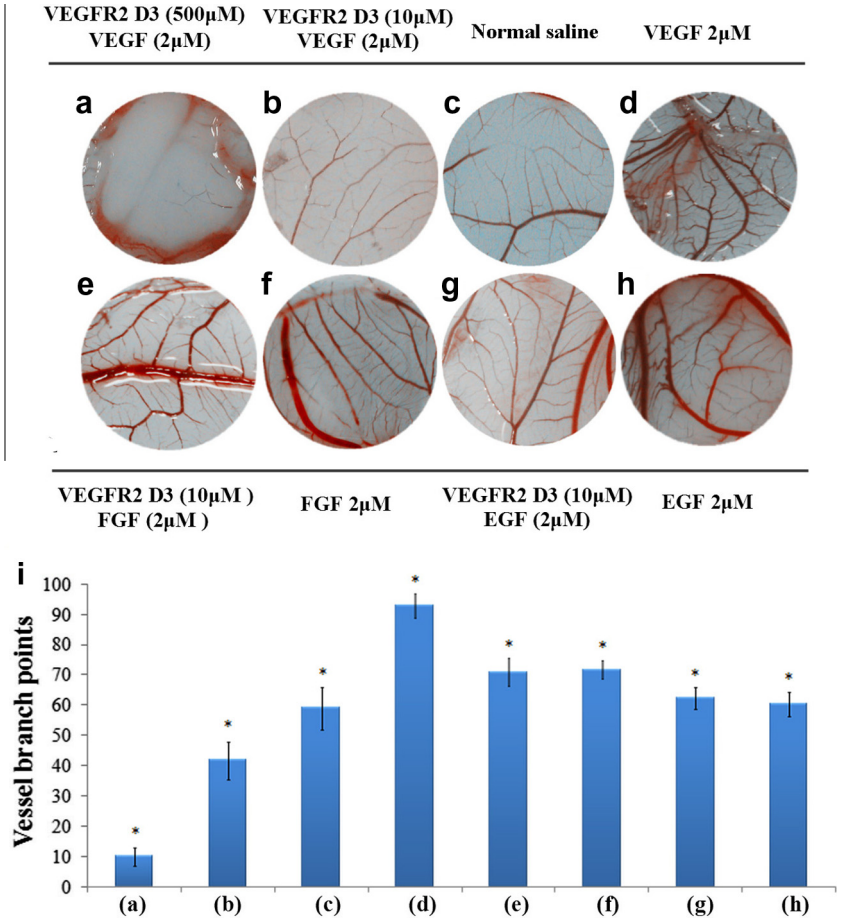

Fig. 10. Antiangiogenesis activity of VEGFR2 D3 *in vivo*. A filter-paper disk with corresponding sample was placed on chick chorioallantoic membrane. After 48 h, membranes were fixed and photographed. (a–h) Representative photographs of CAM assays. (a) VEGFR2 D3 (500 μM) + VEGF (2 μM), (b) VEGFR2 D3 (10 μM) + VEGF (2 μM), (c) control: physiological saline, (d) VEGF (2 μM), (e) VEGFR2 D3 (10 μM) + FGF (2 μM), (f) FGF (2 μM), (g) VEGFR2 D3 (10 μM) + EGF (2 μM), (h) EGF (2 μM) (i) Quantitative analysis of neovascularization from the photographs. Results are presented as mean ± SD of three assays; ∗ means significant difference in comparison to control group, $p < 0.05$.

The CCD model in this study was then proved to predict the optimization of periplasmic expression for recombinant VEGFR2 D3 in *E. coli* Rosetta-gami (DE3)/pET22b adequately, and the yield was improved by 60%. It is well-known that various by-products and toxicity usually accumulate by the time going. Plus, researchers also reported that the over-high level of nutrients will cause

chance in the percents between different products [22]. Based on these, we proposed that this result was derived from a balance between taking nutrient and producing sundry by-products for *E. coli*.

Furthermore, the other six other factors also proved to be able to influence the periplasmic expression by PBD. For the post-induction temperature, inducing the expression of VEGFR2 D3 at 16 °C increased the yield in our study. Hernandez et al. also reported that lower temperature after induction increased the solubility of recombinant protein, which expressed in the periplasmic space of *E. coli* [27]. The possible reason may lie in that high-temperature could increase hydrophobic interaction and influence the aggregation reaction. Then, adding the ammonium sulfate did not increase the yield of periplasmic expression of VEGFR2 D3. In a contract to our result, Nidhi Pareek et al. proved that ammonium sulfate benefited in the expression of SAEM-51[11]. The possible reason lies in the limitation of periplasmic space, which also decides the yield of periplasmic expression. Plus, when IPTG was used at the concentration of 0.05 mM, the yield of target protein was enhanced. Unlike our result, lots of researchers reported that higher concentration of inducer will result in a higher protein yield. It is probably due to the promoted folding rate of protein. The transportation rate induced by high-level IPTG also leads to the formation of inclusion body and the decrease of the soluble and active protein [31]. The result also showed that glycerin can promote the accumulation of protein in the periplasmic protein, the same as Cofre et al. reported [32]. *E. coli* generates acetic acid as the by-produce, which has several negative influences on protein expression. Glycerin can limit the acetate accumulation and adjust the redox rate within the cytoplasma, increasing the productivity of periplasmic protein. For the rotational speed after induction, the lower speed enhanced the expression level of VEGFR2 D3. Claudia Hartmann et al. also adopted the low rotational speed to enhance the yield of recombinant membrane protein UncI in *E. coli* [28]. Faster speed will bring more oxygen into the culture medium, accelerating the progress of transcription.

Sunitinib (SU11248, Sutent®) is a VEGFR-targeting drug, which inhibits several receptor tyrosine kinases (RTKs), such as VEGFR-1, 2, and 3. It is also known to exhibit a direct anti-proliferative effect *in vitro* and *in vivo* against a variety of cells [33]. So, Sunitinib was taken as the positive control in this paper for VEGF induced proliferation assay and CAM assay. FGF and EGF, as well as VEGF, show angiogenic activity both *in vitro* and *in vivo* [34,35].To demonstrate the functional specificity of the recombinant VEGFR2 D3, FGF and EGF were tested the combination with VEGFR2 D3 in ELISA assay, proliferation assay and CAM assay.

The ligand binding activity of the target protein was tested by ELISA. The data showed that the VEGFR2 D3 could bind to $VEGF_{165}$ in a dose-dependent manner and could not combine with other immobilized ligands, including BSA, EGF, FGF, TNF-α and IFN-γ. These results reflected the specific binding between $VEGF_{165}$ and recombinant VEGFR2 D3. Plus, the VEGF induced proliferation assay also illustrated that VEGFR2 D3 restrained the proliferation of EA.hy926, showing a dose-depended tendency. The potential explanation was VEGF could promote the proliferation of EA.hy926 by interacting with VEGFR2 on the surface of the cells and the recombinant VEGFR2 D3 could neutralize the free VEGF competitively with natural VEGFR2. Therefore, increasing the concentration of VEGFR2 D3 could possibly lead to the increase of the interaction between VEGFR2 D3 and VEGF, which resulted in a decrease of the proliferation-promotion function of VEGF to the EA.hy926 cells. In addition, the grown inhibitory effect of recombinant VEGFR2 D3 was specifically related to VEGF, showing no effect to other angiogenic factors such as FGF and EGF.

Furthermore, we proved the capability of VEGFR2 D3 to suppress new blood vessel formation *in vivo*, using the CAM assay as an angiogenesis model. The conventional methods for studying *in vivo* angiogenesis assay include the hamster check pouch, the rabbit ear chamber, the rodent dorsal skin and air sac, the iris and avascular cornea of the rodent eye, and the CAM assay employed in this study [36]. We settled on the CAM assay because the chick embryo chorioallantoic membrane, as a densely vascularized, extra-embryonic tissue model, is very fast and precise to get the results. It is also able to provide a convenient platform to analyze and study both angiogenesis and anti-angiogenesis [37]. There are different methods to quantify the CAM angiogenic response, including the counting uptake of ^3H thymidine into the whole CAM, observing the distribution of the converging neo vessels, calculating the length, the area and the density of the vessels. In the recent years, counting the vessel branch points, which was adopted in this study, has become a popular quantification method [38]. The results indicated that VEGFR2 D3 was capable of inhibiting neo-vessel formation *in vivo* via combining with VEGF specially rather than other angiogenic factors.

VEGF inhibitors are now in clinical practice and have shown encouraging results, which is manageable and safe as well as active anticancer agents. Compared to other inhibitors, the recombinant VEGFR2 D3 has low molecular mass (15 kDa), which almost 10% of normal antibody drugs in molecular weight. Small size means lower immunologic response and better pharmacokinetics, which can pass the renal filter rapidly, penetrate the tissue fast and clear from blood quickly. However, this feature also stands for a shorter half-life, corresponding to higher dose for usage. The recombinant VEGFR2 D3 also products easily in prokaryotic expression system, which makes the corresponding cost lower than other antibody drugs. However, as one of the VEGF-related angiogenesis inhibitors, VEGFR2 D3 is impossible to completely devoid of toxicity. The reported side-effects of similar inhibitors contain: hypertension and cardiovascular event, myelosuppression, perforations, bleeding, voice changes, neurological complications, mucositis, gastrointestinal, skin toxicity, transaminase elevation, fatigue and hand food syndrome [39]. Fortunately, those side-effects share a recognizable pattern. The reason lies in that the majority of those effects are attributable to the inhibition of VEGF's physiological activity.

In the next work, more assays *in vitro* and *in vivo* will be taken to illustrate the angiogenic inhibition ability of VEGFR2 D3, such as the dorsal skin fold chamber assay, flow cytometry assay, cell adherence assay and so on.

In conclusion, we provide a novel antiangiogenic drug candidate relating to VEGF-VEGFR2 pathway. Furthermore, we also established an effective and reliable methodology to obtain the recombinant protein drug in a prokaryotic system.

Acknowledgments

This project was supported by the National Natural Science Foundation of China (NSFC81072561, NSFC81102364 and NSFC81273425). The Project Program of State Key Laboratory of Natural Medicines(China Pharmaceutical University, JKGP201101); Provincial Science and technology supporting program (BE2009675); Project Blue Engineering; Colleges and Universities in Jiangsu Province Plans to Graduate Research and Innovation Projects (2011 CXZZ11_0818).

Appendix A. Supplementary data

Supplementary data associated with this article can be found, in the online version, at http://dx.doi.org/10.1016/j.pep.2013.04.010.

References

[1] P. Nicholas, M. Joel, R. Qin, R. Ashique, R.P. Michael, S. Ergang, A.P. Erica, D.Y. George, S. Neil, J.W. Stanley, Binding and neutralization of vascular endothelial

growth factor (VEGF) and related ligands by VEGF Trap, ranibizumab and bevacizumab, Angiogenesis 15 (2012) 171–185.
[2] N. Ferrara, H.P. Gerber, J. LeCouter, The biology of VEGF and its receptors, Nat. Med. 9 (2003) 669–676.
[3] G. Fuh, B. Li, C. Crowley, B. Cunningham, J.A. Wells, Requirements for binding and signaling of the kinase domain receptor for vascular endothelial growth factor, J. Biol. Chem. 273 (1998) 11197–11204.
[4] H.R. Dorothy, Z.H. Jian, L.K. Mark, T. Richard, T. Andrea, M.O. Kathleen, Y. Darrell, J.H.S. Charles, J.K. Jessica, Anti-VEGF antibody suppresses primary tumor growth and metastasis in an experimental model of Wilms' tumor, J. Pediatr. Surg. 35 (2000) 30–33.
[5] S.F. Fadi, T. Arafat, F. Najla, M. Rami, K.O. Zaher, S.A. Raafat, H.A. Ahmad, S. Ali, Expression, prognostic and predictive impact of VEGF and bFGF in non-small cell lung cancer, Crit. Rev. Oncol. Hematol. 84 (2012) 149–160.
[6] N. Ferrara, L. Damico, N. Shams, H. Lowman, R. Kim, Development of ranibizumab, an anti-vascular endothelial growth factor antigen binding fragment, as therapy for neovascular agerelated macular degeneration, Retina 26 (2006) 859–870.
[7] K.O. Zaher, A.H. Hassan, M.M. Khaled, H.A. Ahmad, I.S. Ali, Is VEGF a predictive biomarker to anti-angiogenic therapy, Crit. Rev. Oncol. Hematol. 79 (2011) 103–111.
[8] J. Sambrook, Molecular Cloning: A Laboratory Manual, second ed., Cold Spring Harbor, NY, 1989.
[9] N.R. Ramakrishnan, S.T. Joo, S.M. Mohd, C.L. Tau, T.T. Beng, B.A. Arbakariya, Optimization of osmotic shock process variables for enhancement of the release of periplasmic interferon-a2b from *Escherichia coli* using response surface method, Process Biochem. 45 (2010) 196–202.
[10] S.C. Cao, Y. Zhang, F. Liu, Q. Wang, Q.F. Zhang, Q.Z. Liu, C. Li, M.F. Liang, D.X. Li, Secretory expression and purification of recombinant *Escherichia coli* heat-labile enterotoxin B subunit and its applications on intranasal vaccination of hantavirus, Mol. Biotechnol. 41 (2009) 91–98.
[11] P. Nidhi, R.P. Singh, G. Sanjoy, Optimization of medium composition for enhanced chitin deacetylase production by mutant *Penicillium oxalicum* SAEM-51 using response surface methodology under submerged fermentation, Process Biochem. 46 (2011) 1693–1697.
[12] H. Gao, M. Liu, J.T. Liu, H.Q. Dai, X.L. Zhou, X.Y. Liu, Y. Zhuo, W.Q. Zhan, L.H. Zhang, Medium optimization for the production of avermectin B1a by *Streptomyces avermitilis* 14-12A using response surface methodology, Bioresour. Technol. 100 (2009) 4012–4016.
[13] S. Anita, R.B. Narsi, Optimization of ethanol production from microwave alkali pretreated rice straw using statistical experimental designs by *Saccharomyces cerevisiae*, Ind. Crop. Prod. 37 (2012) 334–341.
[14] X. Li, T.C. Xu, X.H. Ma, K.P. Guo, L. Kai, Y.H. Zhao, X.M. Jia, Y. Ma, Optimization of culture conditions for production of *cis*-epoxysuccinic acid hydrolase using response surface methodology, Bioresour. Technol. 99 (2008) 5391–5396.
[15] C.F.V. Souza, S.H. Flôres, M.A.Z. Ayub, Optimization of medium composition for the production of transglutaminase by *Bacillus circulans* BL32 using statistical experimental methods, Process Biochem. 41 (2006) 1186–1192.
[16] C. Li, J.P. Cai, J.S. Geng, Purification, characterization and anticancer activity of a polysaccharide from *Panax ginseng*, Int. J. Biol. Macromol. 51 (2012) 968–973.
[17] M.J. Scerbo, J.B. Mario, J.L. Barra, G.A. Roth, G.M. Clara, Expression of a bioactive fusion protein of *Escherichia coli* heat-labile toxin B subunit to a synapsin peptide, Protein Expr. Purif. 59 (2008) 320–326.
[18] H. Deng, C.L. Yan, T. Xiao, D.F. Yuan, J.H. Xu, Total glucosides of *Paeonia lactiflora* Pall inhibit vascular endothelial growth factor-induced angiogenesis, J. Ethnopharmacol. 127 (2010) 781–785.
[19] Y.C. Hseu, S.C. Chen, W.H. Lin, D.Z. Hung, M.K. Lin, Y.H. Kuo, M.T. Wang, H.J. Chou, L. Wang, H.L. Yang, *Toona sinensis* (leaf extracts) inhibit vascular endothelial growth factor (VEGF)-induced angiogenesis in vascular endothelial cells, J. Ethnopharmacol. 134 (2011) 111–1121.
[20] P. Nidhi, R.P. Singh, G. Sanjoy, Optimization of medium composition for enhanced chitin deacetylase production by mutant *Penicillium oxalicum* SAEM-51 using response surface methodology under submerged fermentation, Bioresour. Technol. 46 (2011) 1693–1697.
[21] S. Anita, R.B. Narsi, Optimization of ethanol production from microwave alkali pretreated rice straw using statistical experimental designs by *Saccharomyces cerevisiae*, Ind. Crop. Prod. 37 (2012) 334–341.
[22] X. Li, T.C. Xu, X.H. Ma, L. Kai, Y.H. Zhao, X.M. Jia, Y. Ma, Optimization of culture conditions for production of *cis*-epoxysuccinic acid hydrolase using response surface methodology, Bioresour. Technol. 99 (2008) 5391–5396.
[23] D.P. Zhang, P.L. Wei, L.M. Fan, High-level soluble expression of hIGF-1 fusion protein in recombinant *Escherichia coli*, Process Biochem. 45 (2010) 1401–1405.
[24] T.L.H. Susan, Bacterial cell disruption: a key unit operation in the recovery of intracellular, Biotechnol. Adv. 9 (1991) 217–240.
[25] H. Gao, M. Liu, J.T. Liu, H.Q. Dai, X.L. Zhou, X.Y. Liu, Y. Zhuo, W.Q. Zhang, L.X. Zhang, Medium optimization for the production of avermectin B1a by *Streptomyces avermitilis* 14-12A using response surface methodology, Bioresour. Technol 100 (2009) 4012–4016.
[26] Z.W. Wang, W.B. Huang, Y.P. Chao, Efficient production of recombinant proteins in *Escherichia coli* using an improved l-arabinose-inducible T7 expression system, Process Biochem. 40 (2005) 3137–3142.
[27] H.V.E. Balderas, L.M.P. Maldonado, E.M. Rivero, A.P.B. Rosa, J.F.J. Bremont, L.G.O. Acevedo, A.D.L. Rodriguez, Periplasmic expression and recovery of human interferon gamma in *Escherichia coli*, Protein Expr. Purif. 59 (2008) 169–174.
[28] C. Hartmanna, A. Engela, Cloning, expression, purification, and characterization of the membrane protein Uncl from *Escherichia coli*, Protein Expr. Purif. 79 (2011) 187–190.
[29] I.H. Cho, K.D. Zoh, Photocatalytic degradation of azo dye (Reactive Red 120) in TiO2/UV system: optimization and modeling using a responsesurface methodology (RSM) based on the central composite design, Dyes Pigments 75 (2007) 533–543.
[30] N. Parisa, K. Khosro, A. Neda, Optimizing of the formation of active BMW-amylase after *in vitro* refolding, Protein Expr. Purif 85 (2012) 18–24.
[31] O.A. Olaofea, G.S. Burtona, A.D. Cowanb, T.L.S. Harrison, Improving the production of a thermostable amidase through optimising IPTG induction in a highly dense culture of recombinant *Escherichia coli*, Biochem. Eng. J. 52 (2010) 19–24.
[32] M.A. Eiteman, E. Altman, Overcoming acetate in *Escherichia coli* recombinant protein fermentations, Trends Biotechnol. 24 (2006) 530–536.
[33] N. Andrae, E. Kirches, R. Hartig, D. Haase, G. Keilhoff, T. Kalinski, C. Mawrin, Sunitinib targets PDGF-receptor and Flt3 and reduces survival and migration of human meningioma cells, Eur. J. Cancer 48 (2012) 1831–1841.
[34] M.T. Conconi, B. Nico, D. Guidolin, S. Baiguera, R. Spinazzi, P. Rebuffat, L.K. Malendowicz, A. Vacca, G. Carraro, P.P. Parnigotto, G.G. Nussdorfer, D. Ribatti, Ghrelin inhibits FGF-2-mediated angiogenesis *in vitro* and *in vivo*, Peptides 25 (2004) 2179–2185.
[35] T. Mochizuki, K. Sakai, M. Iwashita, Effects of insulin-like growth factor (IGF) binding protein-3 (IGFBP-3) on endometrial cancer (HHUA) cell apoptosis and EGF stimulated cell proliferation *in vitro*, Growth Horm. IGF. Res. 16 (2006) 202–210.
[36] D. Ribatti, A. Vacca, M. Bertossi, B.G. De, L. Roncali, F. Dammacco, Angiogenesis induced by B-cell non-Hodgkin's lymphomas. Lack of correlation with tumor malignancy and immunologic phenotype, Anticancer Res. 10 (1990) 401–406.
[37] L. Su, K. Rao, F. Guo, X. Li, A.A. Ahmed, Y. Ni, R. Grossmann, R. Zhao, In ovo leptin administration inhibits chorioallantoic membrane angiogenesis in female chicken embryos through the STAT3-mediated vascular endothelial growth factor (VEGF) pathway, Domest. Anim. Endocrin. 43 (2012) 26–36.
[38] R. Domenico, Chick embryo chorioallantoic membrane as a useful tool to study angiogenesis, Int. Rev. Cell Mol. Biol. 270 (2008) 181–224.
[39] F.A. Eskens, J. Verweij, The clinical toxicity profile of vascular endothelial growth factor (VEGF) and vascular endothelial growth factor receptor (VEGFR) targeting angiogenesis inhibitors, Eur. J. Cancer 42 (2006) 3127–3139.